

Classical Correlations and Quantum Interference in Ballistic Conductors

Daniel Waltner and Klaus Richter

Institut für Theoretische Physik
Universität Regensburg, D-93040 Regensburg, Germany

November 6, 2018

Abstract

We illustrate how classical chaotic dynamics influences the quantum properties at mesoscopic scales. As a model case we study semiclassically coherent transport through ballistic mesoscopic systems within the Landauer formalism beyond the so-called diagonal approximation, *i.e.* by incorporating classical action correlations. In this context we review and explain the two main trajectory-based methods developed for calculating quantum corrections: the configuration space approach and the phase space approach that can be regarded as less illustrative but more general than the first one.

1 Introduction: quantum transport through chaotic conductors

Among the most important properties characterizing an electronic nanosystem is its electrical conductance behavior. Hence gaining knowledge on charge transport mechanisms, in particular when shrinking conductors from macroscopic sizes down to molecular-sized wires or atomic point contacts, has been in the focus of experimental and theoretical research throughout the last decade. Such a reduction in size and spatial dimensionality goes along with a crossover from charge flow in the macroscopic bulk, well described by Ohm's law, to distinct quantum effects in the limit of microscopic or atomistic wires. Nanoconductors in the crossover regime, often referred to as mesoscopic, frequently exhibit a co-existence of both classical remnants of bulk features, combined with signatures from wave interference. Such quantum effects usually require low temperatures where coherence of the electronic wavefunctions is retained up to micron scales. This has led to the observation of various quantum interference phenomena such as quantized steps in the point contact conductance, the Aharonov-Bohm effect and universal conductance fluctuations, to name only a few.

Nonlinear effects can enter into transport through mesoscopic or nano-systems twofold: First, as nonlinear I-V characteristics and charge flow far from equilibrium for large enough voltage applied. Second, in the limit of linear response to an applied electric field, the intrinsic nonlinear classical dynamics of the unperturbed conductor can govern its transport properties. In this chapter we focus

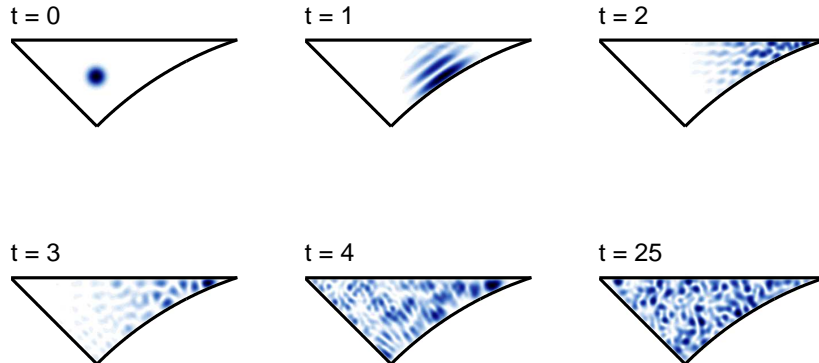


Figure 1: Quantum mechanical wave packet launched into a mesoscopic cavity with the geometry of a "desymmetrized diamond billiard". The wave packet evolution is monitored at times $t = 1, 2, 3, 4,$ and $25,$ in units of the average time between collisions with the walls of a corresponding classical particle (Courtesy of A. Goussev).

on the latter case which is particularly interesting for mesoscopic conductors because the nonlinear charge carrier dynamics can influence both the classical and, in a more subtle way, the quantum transport phenomena.

Initially, disordered metals with underlying diffusive charge carrier motion were in the focus of interest in mesoscopic matter. Here, we instead address ballistic nano- or mesoscopic conductors where impurity scattering is suppressed. The most prominent ballistic systems are nanostructures built from high-mobility semiconductor heterostructures, where electrons are confined to two-dimensional, billiard-type cavities of controllable geometry; however, such systems are also realized as atom optics billiards or through wave scattering as optical, microwave, or acoustic mesoscopic resonators [1].

The quantum dynamics of a single particle in such a geometry is illustrated in Fig. 1 showing snapshots of a wave packet after multiples of the average classical time between bounces off the billiard walls. The quantum evolution in such a mesoscopic geometry, with corresponding chaotic classical dynamics, is characterized by two main features: The rapid transition from wave packet motion following roughly the path of a classical particle to random wave interference at larger times and, second, the emergence of wave functions of complex morphology with wave lengths much shorter than the system size. The latter can be used to further specify mesoscopic matter, *i.e.* quantum coherent systems where the smallest (quantum) length scale, the de Broglie wave length or Fermi wave length λ_F in electronic conductors, is much smaller than the system size \mathcal{L} , *i.e.* $1/(k_F \mathcal{L})$ is a small parameter, in terms of the Fermi momentum $k_F = 2\pi/\lambda_F$, but not fully negligible as in the case of macroscopic systems.

Such ballistic mesoscopic systems are ideal tools to study the connection between (chaotic) classical dynamics and wave interference. Semiclassical techniques provide this link presumably in the most direct way. Modern semiclassical theory is based on trace formulas, sums over Fourier-type components associated with classical trajectories. Analogous to the famous Gutzwiller trace formula for the density of states [2], there exist corresponding expressions for quantum

transport in the linear response regime. There, semiclassical expressions for the conductance have been obtained within the framework of the Landauer-Büttiker approach, relating conductance to quantum transmission in nanostructures.

After early, pioneering semiclassical work by Miller [3] for molecular reactions and later by Blümel and Smilansky [4] for quantum chaotic scattering, major advances were made in the context of mesoscopic conductance in the early nineties by Baranger, Jalabert and Stone [5, 6]. All these semiclassical approaches were based on, and limited by, the so-called diagonal approximation, see below. While most of the features of experimental and numerical magneto-conductance profiles could be well explained qualitatively on the level of the diagonal approximation, it contained the major drawback that it was not current-conserving and hence failed to give correct quantitative predictions for the quantum transmission. This was cured about 10 years later when an approach was devised to account for off-diagonal contributions to the semiclassical conductance [7], thereby achieving unitarity, reflected in (average) current conservation, and furthermore agreement with existing predictions from random matrix theory (RMT). The applicability of RMT to closed chaotic mesoscopic systems was conjectured after numerical simulations in [8]. So it was expected to be applicable also to open systems.

Semiclassical ballistic transport on the level of the diagonal approximation was reviewed in detail in Refs. [9, 10, 11]. In this chapter we hence focus on recent progress beyond the diagonal approximation during the last years. This serves as a model case which illustrates how chaotic nonlinear dynamics can govern quantum properties at nanoscales.

2 Semiclassical limit of the Landauer transport approach

The Landauer formalism [12], providing a link between the quantum transmission and conductance, has proven to be an appropriate framework to address phase-coherent transport through nanosystems. Consider a sample attached to two leads of width W_1 and W_2 that support N_1 , respectively, N_2 current carrying transverse modes at (Fermi-)energy E_F . For such a two-terminal setup the conductance reads at very low temperatures [12]

$$G(E_F) = g_s \frac{e^2}{h} T(E_F) = g_s \frac{e^2}{h} \sum_{m=1}^{N_1} \sum_{n=1}^{N_2} |t_{nm}(E_F)|^2 \quad (1)$$

with $N_1 = W_1 \sqrt{2mE_F}/(\hbar\pi)$ and an analogous relation for N_2 . Here, $g_s = 2$ accounts for spin degeneracy, and the $t_{nm}(E)$ are transmission amplitudes between incoming channels m and outgoing channels n in the leads at energy E . They can be expressed in terms of the projections of the Green function of the scattering region onto the transverse modes $\phi_n(y')$ and $\phi_m(y)$ in the two leads [13]:

$$t_{nm}(E) = -i\hbar(v_n v_m)^{1/2} \int dy' \int dy \phi_n^*(y') \phi_m(y) G(x', y', x, y; E). \quad (2)$$

Here x and x' , respectively, denote the direction along the leads and v_n, v_m the corresponding longitudinal velocities. The integrals in Eq. (2) are taken over

the cross sections of the (straight) leads at the entrance and the exit.

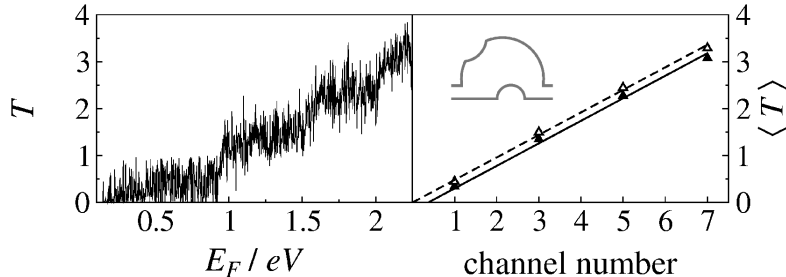


Figure 2: Total quantum transmission (as a function of energy E_F , on the right in units of the channel number in the leads of width $W_1 = W_2 = W$) for transport through a phase-coherent graphene-based quantum dot, see inset. The fluctuating line in the left panel is the full quantum transmission at zero magnetic field. In the right panel, the straight solid and dashed line denote the averaged transmission at zero magnetic field and a magnetic field corresponding to a flux $\phi = 1.6\phi_0$ with the flux quantum $\phi_0 = hc/e$. The difference marks the weak localization correction (from Ref. [14]).

Fig. 2 shows the quantum transmission, numerically obtained from Eq. (2), for a "graphene billiard" [14], fabricated by cutting a cavity out of a two-dimensional graphene flake, a monoatomic layer of carbon atoms arranged in a honeycomb lattice. Two major quantum features are visible: (i) distinct "ballistic conductance fluctuations" as a function of energy. (ii) When subject to an additional, perpendicular magnetic field B with magnetic flux ϕ , the average transmission (straight dashed line in the right panel) shows a small positive offset compared to the average transmission for $B = 0$ (solid line). This reduction of the average conductance at zero magnetic field reflects a weak-localization effect [15]. Its origin is non-classical and due to wave interference.

Here we focus on this ballistic weak localization effect and present its semiclassical derivation for conductors with classically chaotic analogue. The semiclassical approximation enters in two steps: First, we replace $G(x', y', x, y; E)$ in Eq. (2) by the semiclassical Green function (in two dimensions) [2]:

$$G^{\text{sc}}(\mathbf{r}', \mathbf{r}; E) = \frac{1}{i\hbar(2i\pi\hbar)^{1/2}} \sum_t D_t(\mathbf{r}', \mathbf{r}) \exp\left(\frac{i}{\hbar}S_t - i\eta_t \frac{\pi}{2}\right). \quad (3)$$

It is given as a sum over contributions from all classical trajectories t connecting the two fixed points \mathbf{r} and \mathbf{r}' at energy E . In Eq. (3),

$$S_t(\mathbf{r}', \mathbf{r}; E) = \int_{\mathcal{C}_t} \vec{p} \cdot d\vec{q} \quad (4)$$

is the classical action along a path \mathcal{C}_t between \mathbf{r} and \mathbf{r}' and governs the accumulated phase.

Second, we evaluate the projection integrals in Eq. (2) for isolated trajectories within the stationary-phase approximation. For leads with hard-wall boundaries the mode wavefunctions are sinusoidal, $\phi_m(y) = \sqrt{2/W_1} \sin(m\pi y/W_1)$.

Hence the stationary-phase condition for the y integral requires [9]

$$\left(\frac{\partial S}{\partial y}\right)_{y'} = -p_y \equiv -\frac{\bar{m}\hbar\pi}{W_1}, \quad (5)$$

with $\bar{m} = \pm m$. The stationary-phase solution of the y' integral yields a corresponding ‘‘quantization’’ condition for the transverse momentum $p_{y'}$. Thus only those paths which enter into the cavity at (x, y) with a fixed angle $\sin\theta = \pm m\pi/kW_1$ and exit the cavity at (x', y') with angle $\sin\theta' = \pm n\pi/kW_2$ contribute to $t_{nm}(E)$ with $k = \sqrt{2mE}/\hbar$. There is an intuitive explanation: the trajectories are those whose transverse wave vectors on entrance and exit match the wave vectors of the modes in the leads. One then obtains for the semiclassical transmission amplitudes

$$t_{nm}(k) = -\frac{\sqrt{2\pi i\hbar}}{2\sqrt{W_1 W_2}} \sum_{t(\bar{n}, \bar{m})} \text{sgn}(\bar{n}) \text{sgn}(\bar{m}) \sqrt{A_t} \exp\left[\frac{i}{\hbar}\tilde{S}_t(\bar{n}, \bar{m}; k) - i\frac{\pi}{2}\tilde{\mu}_t\right]. \quad (6)$$

Here, the reduced actions are

$$\tilde{S}_t(\bar{n}, \bar{m}; k) = S_t(k) + \hbar k y \sin\theta - \hbar k y' \sin\theta', \quad (7)$$

which can be considered as Legendre transforms of the original action functional. The phases $\tilde{\mu}_t$ contain both the usual Morse indices and additional phases arising from the y, y' integrations. The prefactors are $A_t = |(\partial y/\partial\theta')_\theta|/(\hbar k |\cos\theta'|)$. The resulting semiclassical expression for the transmission and thereby the conductance (see Eq. (1)) in chaotic cavities involves contributions from pairs of trajectories t, t' . It reads [5, 6, 9]

$$T(k) = \sum_{m=1}^{N_1} \sum_{n=1}^{N_2} |t_{nm}(k)|^2 = \frac{\pi\hbar}{2W_1 W_2} \sum_{m=1}^{N_1} \sum_{n=1}^{N_2} \sum_{t, t'} F_{n, m}^{t, t'}(k) \quad (8)$$

with

$$F_{n, m}^{t, t'}(k) \equiv \sqrt{A_t A_{t'}} \exp\left[\frac{i}{\hbar}(\tilde{S}_t - \tilde{S}_{t'}) - i\mu_{t, t'}\frac{\pi}{2}\right], \quad (9)$$

where the phase $\mu_{t, t'}$ accounts for the differences of the phases $\tilde{\mu}_t$ and the sgn factors in Eq. (6).

In the next two sections we show how one can calculate with purely semiclassical methods quantum corrections to the transmission beyond the diagonal approximation. The results obtained for chaotic conductors are consistent with RMT-predictions.

3 Quantum transmission: configuration space approach

In evaluating the off-diagonal (interference) contributions to the quantum transmission we present two approaches. The first approach is based on the analysis of off-diagonal pairs of trajectories and their self-intersections in configuration space. This approach is more illustrative, but less general than the second, phase space approach outlined in Sec. 4.

We start from the semiclassical expression for $|t_{nm}(k)|^2$ obtained by squaring the semiclassical transmission amplitudes, Eq. (6), see also Eqs. (8,9):

$$|t_{nm}(k)|^2 = \frac{\pi\hbar}{2W_1W_2} \sum_{t,t'} \sqrt{A_t A_{t'}} \exp \left[\frac{i}{\hbar} (\tilde{S}_t - \tilde{S}_{t'}) - i\mu_{t,t'} \frac{\pi}{2} \right]. \quad (10)$$

Due to the action difference of the trajectories t and t' in the exponential in Eq. (10), this expression is a rapidly oscillating function of k or the energy in the semiclassical limit of large ratios $(S_t - S_{t'})/\hbar$. In the following we wish to identify those contributions to Eq. (10) which survive an average over a classically small but quantum mechanically large k -window Δk . Such contributions must come from very similar trajectories. Afterwards we wish to evaluate their contributions to $|t_{nm}(k)|^2$ using basic principles of chaotic dynamics: for our calculation we will need hyperbolicity and ergodicity. Hyperbolicity implies the possible exponential separation of neighboring trajectories for long times with the distance growing proportional to $e^{\lambda T}$, with the Lyapunov exponent λ and the time T of the trajectory. The second principle, ergodicity, means the equidistribution of long trajectories on the energy surface at the energy E of the trajectory.

This section is divided into four subsections: after calculating the diagonal contribution we determine the simplest nondiagonal contribution in the second part. The behavior of the latter as a function of a magnetic field and a finite Ehrenfest time is then studied in the third and fourth subsection, respectively.

3.1 Diagonal contribution

The first, "diagonal" (D) contribution to Eq. (10) originates from identical trajectories $t = t'$, meaning $S_t = S_{t'}$. It gives

$$|t_{nm}(k)|_D^2 = \frac{\pi\hbar}{2W_1W_2} \sum_t A_t. \quad (11)$$

The remaining sum over classical trajectories in Eq. (11) can be calculated using a classical sum rule [7] that can be derived using ergodicity, see for example [16]. It yields

$$\sum_t A_t = \frac{4W_1W_2}{\Sigma(E)} \int_0^\infty \rho(T), \quad (12)$$

where $\Sigma(E)$ denotes the phase space volume of the system at energy E , and $\rho(T)$ is the classical probability to find a particle still inside an open system after a time T . For long times the latter decays for a chaotic system exponentially $\rho(T) \sim e^{-T/\tau_D}$, with the dwell time $\tau_D = \frac{\Sigma(E)}{2\pi\hbar(N_1+N_2)}$. This exponential decay can be easily understood based on the equidistribution of trajectories: the number ΔN of particles leaving the system during ΔT is given by the overall number of particles N times the ratio of the phase space volume from which the particles leave during ΔT and the whole phase space volume of the system. The differential equation for N , obtained in the case of infinitesimal ΔT , has obviously an exponential solution.

By inserting Eq. (12) into Eq. (11), we obtain

$$|t_{nm}(k)|_D^2 = \frac{1}{N_1 + N_2}. \quad (13)$$

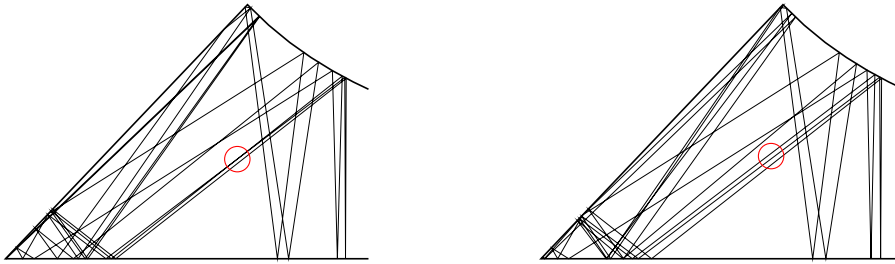


Figure 3: Pair of two periodic orbits in the hyperbola billiard differing from each other essentially in the region marked by the circle, where the left orbit exhibits a self-crossing while the right partner orbit shows an "avoided crossing" (Courtesy of M. Sieber).

Its derivation required ergodicity valid only for long trajectories. We will assume that the classical dwell time is large enough, in order to have a statistically relevant number of long trajectories left after time t . The result in Eq. (13) allows for a very simple interpretation: It is just the probability of reaching one of the $N_1 + N_2$ channels if each of the channels can be reached equally likely.

3.2 Nondiagonal contribution

In the following we will calculate the contributions from pairs of different trajectories, however with similar actions. For a long time it was not clear how these orbits could look like. There are many orbit pairs in a chaotic system having accidentally equal or nearly equal actions. However, in order to describe universal features of a chaotic system after energy averaging, one has to find orbits that are correlated in a systematic way. These orbits were first identified and analyzed in 2000 in the context of spectral statistics [17]. There, *periodic* orbits were studied to compute correlations between energy eigenvalues of quantum systems with classically chaotic counterpart. Based on *open*, lead-connecting trajectories, in Ref. [7] this approach was generalized to the conductance we study here. Still, the underlying mechanism to form pairs of classically correlated orbits is the same in the two cases.

In Fig. 3 we show a representative example of such a correlated (periodic) orbit pair in the chaotic hyperbola billiard. The two partner orbits are topologically the same up to the region marked by the circle where one orbit exhibits a self-crossing (left panel) while the partner orbit an 'avoided' crossing (right panel). Usually, such trajectory pairs are drawn schematically as shown in Fig. 4.

One considers very long orbits with self-crossings characterized by crossing angles $\epsilon \ll \pi$. In Ref. [17] it was shown that there exists for each orbit a partner orbit starting and ending (exponentially) close to the first one. It follows the first orbit until the crossing, avoids this, however, traverses the loop in reversed direction and avoids the crossing again.

In order to quantify the contribution of these trajectory pairs to Eq. (10) we need two inputs: an expression for the action difference and for the density quantifying how often an orbit of time T exhibits a self-intersection, both quantities expressed as a function of the parameter ϵ . The formula for the action

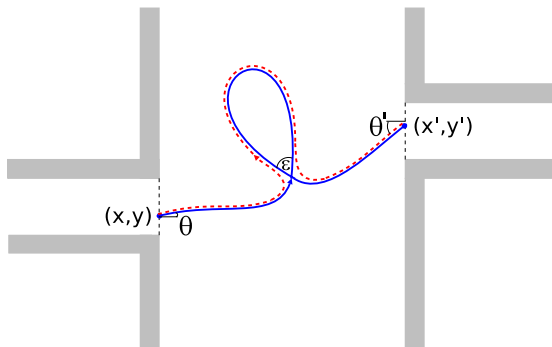


Figure 4: Schematic drawing of a pair of orbits yielding the first nondiagonal contribution to the transmission considered in Ref. [7]. One of the orbits crosses itself under an angle ϵ , the other one possesses an "avoided crossing". Except for the crossing region both orbits are almost identical.

difference ΔS can be derived by linearizing the dynamics of the orbit without crossing around the reference orbit with crossing, giving, in the limit $\epsilon \ll \pi$, [17]

$$\Delta S = \frac{p^2 \epsilon^2}{2m\lambda}. \quad (14)$$

At this point we can justify our assumption of small crossing angles ϵ : In the limit $\hbar \rightarrow 0$, we expect important contributions to Eq. (10) only from orbit pairs with small action differences, *i.e.* small crossing angles, as we see from Eq. (14).

Before deriving the number of self-crossings, $P(\epsilon, T) d\epsilon$, in the range between ϵ and $\epsilon + d\epsilon$ of an orbit of time T , we give rough arguments how this expression depends on ϵ and T for trajectories in billiards. There, each orbit is composed of a chain of N chords connecting the reflection points. Following an orbit, the first two chords cannot intersect, the third chord can cross with up to one, the fourth chord with up to two segments, and so on. Hence, the overall number of self-crossings will be proportional to $\sum_{n=3}^N (n-2) \propto N^2$, to leading order in N , *i.e.* proportional to T^2 .

The crossing angle dependence of $P(\epsilon, T)$ can be estimated for small ϵ as follows: Given a trajectory chord of length L , a second chord, tilted by an angle ϵ with respect to the first one, will cross it inside the billiard (with area of order L^2) only if the distance between the reflection points of the two chords at the boundary is smaller than $L \sin \epsilon$. The triangle formed in the latter case includes a fraction $\sin \epsilon$ of the entire billiard size. From this rough estimation we expect $P(\epsilon, T) \propto T^2 \sin \epsilon$.

More rigorously, the quantity $P(\epsilon, T) d\epsilon$, can be expressed for an arbitrary orbit γ as [17]

$$P(\epsilon, T) d\epsilon = \left\langle \int_{T_{\min}(\epsilon)}^{T-T_{\min}(\epsilon)} dt_l \int_{T_{\min}(\epsilon)/2}^{T-t_l-T_{\min}(\epsilon)/2} dt_s |J| \delta(\mathbf{x}(t_s) - \mathbf{x}(t_s + t_l)) \times \delta(\epsilon - \alpha(t_s, t_s + t_l)) \right\rangle d\epsilon \quad (15)$$

with the average $\langle \dots \rangle$ taken over different initial conditions $(\mathbf{x}_0, \mathbf{p}_0)$. The time of the closed loop of the trajectory is denoted by t_l and the time before the

loop by t_s . $\alpha(t_s, t_s + t_l)$ denotes the absolute value of the angle between the velocities $\mathbf{v}(t_s)$ and $\mathbf{v}(t_s + t_l)$. $|J|$ is the Jacobian for the transformation from the argument of the first delta function to t_l and t_s ensuring that $P(\epsilon, T) d\epsilon$ yields a 1 for each crossing of γ . With the absolute value of the velocity, v , it can be expressed as

$$|J| = |\mathbf{v}(t_s) \times \mathbf{v}(t_s + t_l)| = v^2 \sin \alpha(t_s, t_s + t_l). \quad (16)$$

As the derivation [17] of the formula for $P(\epsilon, T)$ for a chaotic system, starting from the formal expression (15), is instructive to see how information can be extracted from the basic principles of chaotic dynamics beyond the diagonal approximation, we will present it here in detail. Hyperbolicity will yield a justification for the minimal time $T_{\min}(\epsilon)$ already introduced in Eq. (15); we will come back to that point later and first study the effect of ergodicity.

To proceed we interchange the phase space integral of the average with the time integrals, substitute $(\mathbf{x}(t_s), \mathbf{p}(t_s)) \mapsto (\mathbf{x}_0, \mathbf{p}_0)$ in Eq. (15) and obtain

$$P(\epsilon, T) = 2m \int_{T_{\min}(\epsilon)}^{T - T_{\min}(\epsilon)} dt_l v^2 \sin \epsilon p_E(\epsilon, t_l) (T - t_l - T_{\min}(\epsilon)), \quad (17)$$

with the averaged classical return probability density

$$p_E(\epsilon, t_l) = \frac{1}{2m} \langle \delta(\mathbf{x}_0 - \mathbf{x}(t_l)) \delta(\epsilon - |\angle(\mathbf{v}_0, \mathbf{v}(t_l))|) \rangle. \quad (18)$$

This yields the probability density that a particle possessing the energy E returns after the time t_l to its starting point with the angle $|\angle(\mathbf{v}_0, \mathbf{v}(t_l))| = \epsilon$. For long times this can be replaced by $1/\Sigma(E)$, assuming ergodicity. Then we obtain

$$\begin{aligned} P(\epsilon, T) &= 2m \int_{T_{\min}(\epsilon)}^{T - T_{\min}(\epsilon)} dt_l v^2 \sin \epsilon \frac{1}{\Sigma(E)} (T - t_l - T_{\min}(\epsilon)) \\ &= \frac{mv^2}{\Sigma(E)} \sin \epsilon (T - 2T_{\min}(\epsilon))^2. \end{aligned} \quad (19)$$

Now we return to our assumption of hyperbolicity and explain the cutoff time $T_{\min}(\epsilon)$, introduced in the equations above. To this end, we consider two classical paths leaving their crossing with a small angle ϵ . The initial deviation of their velocities is $\delta v_i = \epsilon v$. In order to form a closed loop, the deviation of the velocities δv_f , when both paths have traversed half of the closed loop, has to be given by $\delta v_f = c v$ with c of the order unity. Then we get for the minimal time $T_{\min}(\epsilon)$ to form a closed loop, due to the exponential divergence of neighboring orbits,

$$c = \epsilon e^{(\lambda T_{\min}(\epsilon))/2}, \quad (20)$$

implying

$$T_{\min}(\epsilon) = \frac{2}{\lambda} \ln \left(\frac{c}{\epsilon} \right). \quad (21)$$

An argument similar to the one used here for the closed loop can also be applied to the other two parts of the trajectory leaving the crossing with an angle ϵ towards the opening of the conductor. Suppose t_s has a length between 0 and $T_{\min}(\epsilon)/2$, then both parts have to be so close together that they must leave

both through the same lead. As we are interested in the transmission, we also have to exclude that case¹. A similar argument holds for the case where the last part of the orbit has a length between 0 and $T_{\min}(\epsilon)/2$, in this case the orbit has to come very close to the opening already before the crossing and leave before it could have crossed. Accounting for all these restrictions, gives the integration limits in Eq. (15).

Now we are prepared to calculate the contribution of the considered trajectory pairs to the transmission. Therefore we keep in Eq. (10) one sum over trajectories that we will perform using the same classical sum rule as in diagonal approximation, the other we can replace by a sum over all the partner trajectories of one trajectory, which can be calculated using $P(\epsilon, T)$. There is, however, one subtlety concerning the survival probability $\rho(T)$ in the sum rule: we argued already, that if the crossing happens near the opening, both parts of the orbit act in a correlated way; $\rho(T)$ is changed in the case of the trajectory pairs considered here for a similar reason: because we know that the two parts of the orbit leaving the crossing on each side are very close to each other, the orbit can either leave the cavity during the first stretch, *i.e.* during the first time it traverses the crossing region, or cannot leave at all. This implies that we have to change the survival probability from $\rho(T)$ to $\rho(T - T_{\min}(\epsilon))^2$. Then we arrive at the loop (L) contribution

$$\begin{aligned}
|t_{nm}(k)|_L^2 &= \frac{\pi\hbar}{2W_1W_2} \sum_t \sum_P A_t 2\Re \exp\left(i\frac{p^2\epsilon_P^2}{2m\lambda\hbar}\right) \\
&= \frac{4\pi\hbar}{\Sigma(E)} \int_0^\pi d\epsilon \int_{2T_{\min}(\epsilon)}^\infty dT e^{-(T-T_{\min}(\epsilon))/\tau_D} P(\epsilon, T) \cos\left(\frac{p^2\epsilon^2}{2m\lambda\hbar}\right) \\
&= \frac{8\pi\hbar m v^2 \tau_D^3}{\Sigma(E)^2} \int_0^\pi d\epsilon e^{-T_{\min}(\epsilon)/\tau_D} \sin\epsilon \cos\left(\frac{p^2\epsilon^2}{2m\lambda\hbar}\right) \quad (22)
\end{aligned}$$

with the sum over the partner trajectories P in the first line. As the important contributions require very small action differences, *i.e.* very similar trajectories, and as the prefactor A_t is not as sensitive as the actions to small changes of the trajectories, we can neglect differences between t and t' in the prefactor. In the second line we applied the classical sum rule with the modification explained before Eq. (22) and used $P(\epsilon, T)$ to evaluate the sum over P . After performing the simple time integral in the third line, we can do the ϵ -integration as for example in Ref. [18] by taking into account that the important contributions

¹If we would calculate the reflection instead of the transmission, the effect of short legs, referred to as coherent backscattering, has to be taken into account.

²This effect together with the requirement of a finite length of the orbit parts leaving towards the opening was originally not taken into account in Ref. [7]. In this calculation, the contributions from these two effects cancel each other, they will be only important when considering more complicated diagrams as in the next section.

come from very small ϵ , yielding

$$\begin{aligned}
|t_{nm}(k)|_L^2 &= \frac{8\pi\hbar m v^2 \tau_D^3}{\Sigma(E)^2} \int_0^\pi d\epsilon (\epsilon/c)^{\frac{2}{\lambda\tau_D}} \sin \epsilon \cos\left(\frac{p^2 \epsilon^2}{2m\lambda\hbar}\right) \\
&= \frac{8\pi\hbar m v^2 \tau_D^3}{\Sigma(E)^2} \int dz \frac{m\lambda\hbar}{p^2} \left(\frac{1}{c}\right)^{\left(\frac{2}{\lambda\tau_D}\right)} \left(\frac{2m\lambda\hbar z}{p^2}\right)^{\frac{1}{\lambda\tau_D}} \cos z \\
&= -\frac{8\pi\hbar m v^2 \tau_D^2}{\Sigma(E)^2} \int dz \frac{m\hbar}{p^2} \left(\frac{1}{c}\right)^{\left(\frac{2}{\lambda\tau_D}\right)} \left(\frac{2m\lambda\hbar z}{p^2}\right)^{\frac{1}{\lambda\tau_D}} \frac{\sin z}{z}. \quad (23)
\end{aligned}$$

In the first line we already rewrote $e^{-T_{\min}(\epsilon)/\tau_D}$ as $(\epsilon/c)^{\frac{2}{\lambda\tau_D}}$, and in the second line we approximated $\sin \epsilon \approx \epsilon$ and substituted $z = p^2 \epsilon^2 / (2m\lambda\hbar)$. Then we perform a partial integration with respect to z neglecting rapidly oscillating terms that are cancelled by the k -average, introduced after Eq. (10). Eventually, we perform the z -integral by pushing the upper limit to infinity, *i.e.* $\hbar \rightarrow 0$ and taking into account our assumption of large dwell times, *i.e.* $\lambda\tau_D \rightarrow \infty$. Additionally we assume $(2m\lambda\hbar/p^2)^{\frac{1}{\lambda\tau_D}} \approx 1$; we will return to the last point soon.

Finally, we arrive at the leading nondiagonal contribution to the quantum transmission [7],

$$|t_{nm}(k)|_L^2 = -\frac{1}{(N_1 + N_2)^2}. \quad (24)$$

3.3 Magnetic field dependence of the nondiagonal contribution

Up to now we assumed time reversal symmetry. If this symmetry is destroyed, for example by applying a strong magnetic field, the latter contribution will vanish, because the closed loop has to be traversed in different directions by the trajectory and its partner. Here we study the transition region between zero and finite magnetic field. In particular, we assume a homogeneous magnetic field B_z perpendicular to the sample that is assumed weak enough not to change the classical trajectories, but only the actions in the exponents. Since the closed loop is traversed in different directions by the two trajectories, we obtain an additional phase difference $(4\pi AB_z/\phi_0)$ between the two trajectories with the enclosed area A of the loop and the flux quantum $\phi_0 = (hc/e)$. We further need the distribution of enclosed areas for a trajectory with a closed loop of time T in chaotic systems, given by

$$P(A, T) = \frac{1}{\sqrt{2\pi T\beta}} \exp\left(-\frac{A^2}{2T\beta}\right) \quad (25)$$

with a system specific parameter β . A derivation of this formula can be found for example in Ref. [19]. Including the phase difference and the area distribution

in a modified $P(\epsilon, T)$ yields

$$\begin{aligned}
P_B(\epsilon, T) &= \frac{2mv^2}{\Sigma(E)} \sin \epsilon \int_{T_{\min}(\epsilon)}^{T-T_{\min}(\epsilon)} dt_l (T - t_l - T_{\min}(\epsilon)) \\
&\quad \times \int_{-\infty}^{\infty} dAP(A, t_l - T_{\min}(\epsilon)) \cos \frac{4\pi AB_z}{\Phi_0} \\
&= \frac{2mv^2}{\Sigma(E)} \sin \epsilon \int_{T_{\min}(\epsilon)}^{T-T_{\min}(\epsilon)} dt_l (T - t_l - T_{\min}(\epsilon)) e^{-(t_l - T_{\min}(\epsilon))/t_B} \quad (26)
\end{aligned}$$

with $t_B = \frac{\phi_0^2}{8\pi^2 \beta B_z^2}$. In the first line we used that paths leaving the crossing to form a closed loop, enclose a negligible flux, as long as they are correlated; for a more detailed analysis see Appendix D of Ref. [20]. Performing the T - and ϵ -integrals similar to the case without magnetic field, yields [7]

$$|t_{nm}(k, B_z)|_L^2 = -\frac{1}{(N_1 + N_2)^2} \frac{1}{1 + \tau_D/t_B}. \quad (27)$$

We obtain an inverted Lorentzian with minimum at zero magnetic field, implying that the transmission through our sample increases with increasing magnetic field. This weak localization phenomenon, a precursor of strong localization, is visible as the reduction of the average quantum transmission in Fig. 2.

3.4 Ehrenfest time dependence of the nondiagonal contribution

This semiclassical approach can also be applied to calculate the Ehrenfest time dependence of the transmission. The Ehrenfest time $\tau_E \equiv (1/\lambda) \ln(E/(\lambda\hbar))$, more generally a time proportional to $\ln \hbar$ [21], is the time a wave-packet needs to reach a size such that it can no longer be described by a single classical particle. The Ehrenfest time thus separates the evolution of wave packets following essentially the classical dynamics (e.g. up to few bounces of the wave packet in Fig. 1) from longer time scales dominated by wave interference (last panel in Fig. 1). Based on field theoretical methods, Aleiner and Larkin showed, that a minimal time is required for quantum effects in the transmission to appear, the Ehrenfest time [22]. We will now apply our semiclassical methods to determine the Ehrenfest-time dependence of the transmission following the pioneering work [23] that has later been extended to the reflection [24, 25, 20], including a distinction between different Ehrenfest times. To this end, we directly start from Eq. (22); however, we have to be more careful when evaluating the ϵ -integral: in our former calculation we assumed $e^{-\tau_E/\tau_D} = (\lambda\hbar/E)^{\frac{1}{\lambda\tau_D}} \approx 1$, requiring $\tau_E \ll \tau_D$. Lifting however this strong restriction for τ_D , but still keeping it large enough to fulfill our assumption of chaotic dynamics, we obtain

$$|t_{nm}(k, \tau_E)|_L^2 = -\frac{1}{(N_1 + N_2)^2} e^{-\tau_E/\tau_D}, \quad (28)$$

i.e. an exponential suppression of the nondiagonal contribution due to the Ehrenfest time. This dependence has been confirmed in numerical simulations for quantum maps.

After this introduction into semiclassical methods for the evaluation of non-diagonal contributions in configuration space, we will now turn to the generalization to phase space which also allows for an elegant way to compute higher-order corrections to the leading weak localization contribution presented above.

4 Quantum transmission: phase space approach

The above configuration space treatment, based on self-crossings, is restricted to systems with two degrees of freedom. More generally, for higher-dimensional dynamical systems one cannot assume to find a one-to-one correspondence between partner orbits and crossings of an orbit [26]. In order to overcome these difficulties, a phase space approach was developed for calculating the spectral form factor in spectral statistics in [26, 27] involving periodic orbits. The next challenge was the generalization of this theory to trajectory pairs differing from each other at several places, solved again first for the spectral form factor [28] and generalized to the transport situation considered here in Ref. [29] which serves as the basis of the following discussion.

In this section we first explain the phase space approach and use it afterwards in the way developed in Refs. [28, 29] for the calculation of the quantum transmission involving also higher-order semiclassical diagrams.

4.1 Phase space approach

Compared to the last section, we first of all have to replace the role of the reference orbit. Whereas we used there the crossing orbit as reference and calculated then the action difference and the crossing angle distribution in terms of the crossing angle ϵ , we will consider here the orbit without the crossing that is close to itself in the region, where the partner orbit crossed itself in the last section. Inside the region, where the orbit is close to itself; we will refer to it as encounter region and to the parts of the orbit inside as encounter stretches, that are connected by so called links; we place a so called Poincaré surface of section \mathcal{P} with its origin at $\tilde{x} = (\mathbf{x}, \mathbf{p})$. The section consists of all points $\tilde{x} + \delta\tilde{y} = (\mathbf{x} + \delta\mathbf{x}, \mathbf{p} + \delta\mathbf{p})$ in the same energy shell as the reference point with the $\delta\mathbf{x}$ perpendicular to the momentum \mathbf{p} of the trajectory. For the two-dimensional systems considered here \mathcal{P} is a two-dimensional surface, where every vector $\delta\tilde{y}$ can be expressed in terms of the stable direction $e_s(\tilde{x})$ and the unstable one $e_u(\tilde{x})$ [30]

$$\delta\tilde{y} = se_s(\tilde{x}) + ue_u(\tilde{x}). \quad (29)$$

The expressions stable and unstable refer to the following: we consider two orbits, one starting at \tilde{x} and the other one at $\tilde{x} + \delta\tilde{y}_0$, then the difference between the stable coordinates will decrease exponentially for positive times and increase for negative time exponentially in the limit of long time T , unstable coordinates behave just the other way round. The functional form of the exponentials can be determined as $e^{\lambda T}$ and $e^{-\lambda T}$. Now we can come back to the trajectory with the encounter region, where we have put our Poincaré surface of section. The trajectory considered in the last section will pierce through the Poincaré section twice: one of this points we will consider as the origin of the section

the other piercing will take place at the distance (s, u) . The coordinates of the piercing points of the partner trajectory are determined in the following way: the unstable coordinate of the partner trajectory has to be the same as the one of that part of the first trajectory that the second will follow for positive times. The stable coordinate is determined by the same requirement for negative times.

After this introduction into the determination of the (s, u) -coordinates, we are now ready to treat trajectory pairs that differ in encounters of arbitrary complexity. Following Ref. [29] and using the notation introduced there we will allow here that the two trajectories differ in arbitrarily many encounters involving an arbitrary number of stretches. In order to organize this encounter structure we introduce a vector $\vec{v} = (v_2, v_3, \dots)$ with the component v_l determining the number of encounters with l stretches involved. The overall number of encounters during an orbit will be denoted by $V = \sum_{l=2}^{\infty} v_l$, the overall number of encounter stretches by $L = \sum_{l=2}^{\infty} l v_l$. In an encounter of l stretches, we will get $l - 1$ (s, u) -coordinates.

Now we can proceed by replacing the former expressions for the minimal loop time, the action difference and the crossing angle distribution depending on the former small parameter ϵ , by the corresponding expressions depending on the new small parameters (s, u) .

We start with the minimal loop time, to that one also refers as the duration of the encounter. Shifting the Poincaré surface of section through our encounter, the stable components will asymptotically decrease, the unstable ones will increase for increasing time. We then claim that both components have to be smaller than a classical constant c , its exact value will again, as in the last section, be unimportant for our final results. We finally obtain the encounter duration t_{enc} as the sum of the times t_u , that the trajectory needs from \mathcal{P} till the point where the first unstable component reaches c , and the time t_s , that the trajectory needs from \mathcal{P} till the point where the last stable component falls below c . Thus we get

$$t_{\text{enc}} = t_s + t_u = \frac{1}{\lambda} \ln \frac{c^2}{\max_i \{|s_i|\} \max_j \{|u_j|\}}. \quad (30)$$

Now we treat the action difference between the two trajectories. Expressing the actions of the paired trajectories as the line integral of the momentum along the trajectory, we can expand [26] one action around the other and express the result in terms of the (s, u) -coordinates. This yields for an l -encounter³

$$\Delta S = \sum_{j=1}^{l-1} s_j u_j. \quad (31)$$

The action difference of a trajectory pair is then obtained by adding the differences resulting from all encounters.

Finally we come to the crossing angle distribution that will be replaced here by a weight function for the stable and unstable coordinates for a trajectory of time T . We first notice that the uniformity of the trajectory distribution implies in terms of our coordinates in \mathcal{P} that a trajectory pierces through the section

³Strictly speaking [28] the (s, u) coordinates used here and in the following calculation are for encounters involving more than two stretches *not* the same like the ones described before, but related to them via a linear and volume preserving transformation.

with the coordinates $(u, u + du)$ and $(s, s + ds)$ within the time interval $(t, t + dt)$ with the probability $1/\Sigma(E)dsdu dt$. In general, we obtain for an l -encounter $(1/\Sigma(E))^{l-1} ds^{l-1} du^{l-1} dt^{l-1}$. Integrating the product of the latter quantities for all encounters over all possible durations of the $L - V$ intra-encounter links, in a way that their durations are positive yields our weight function for a fixed position of \mathcal{P} . To take into account all possible positions of \mathcal{P} , we also integrate over all possible positions, where it can be placed and divide by t_{enc} to avoid overcounting of equivalent positions. Taking all link times positive, we obtain for the weight function for an orbit of time T

$$\begin{aligned} w_T(\mathbf{s}, \mathbf{u}) &= \frac{1}{(\Sigma(E))^{L-V} \prod_{\alpha=1}^V t_{\text{enc}}^\alpha} \int_0^\infty dt_1 \dots dt_L \Theta \left(T - \sum_{\alpha=1}^V l_\alpha t_{\text{enc}}^\alpha - \sum_{\alpha=1}^L t_\alpha \right) \\ &= \frac{\left(T - \sum_{\alpha=1}^V l_\alpha t_{\text{enc}}^\alpha \right)^L}{L! (\Sigma(E))^{L-V} \prod_{\alpha=1}^V t_{\text{enc}}^\alpha}. \end{aligned} \quad (32)$$

One additional problem arises, when treating trajectory pairs differing not only in one 2-encounter like in the last section: one can construct for one \vec{v} different trajectory pairs, varying for example in the relative orientation, in which the encounter stretches are traversed. We will count this number by a function $N(\vec{v})$ and describe briefly later, how it can be calculated.

4.2 Calculation of the full transmission

After the introduction into the phase space approach we are now ready to calculate the transmission. Taking the weight function, the action difference and the number of structures, we can transform the non-diagonal (ND) part of Eq. (10) into

$$\begin{aligned} |t_{nm}(k)|_{ND}^2 &= \frac{\pi \hbar}{2W_1 W_2} \sum_t \sum_{\vec{v}} A_t N(\vec{v}) \\ &\times \left\langle \int_{-c}^c \dots \int_{-c}^c d^{L-V} u d^{L-V} s \exp\left(\frac{i}{\hbar} \Delta S\right) w_T(\mathbf{s}, \mathbf{u}) \right\rangle_{\Delta k} \end{aligned} \quad (33)$$

with the average over a small k -window denoted by $\langle \dots \rangle_{\Delta k}$. Inserting the formulas for the action difference, the weight function and using the classical sum rule with the modification of the survival probability, discussed in the last section, we can then transform the integral with respect to the length of the trajectory into one over the last link and obtain

$$\begin{aligned} |t_{nm}(k)|_{ND}^2 &= \frac{2\pi \hbar}{\Sigma(E)} \sum_{\vec{v}} N(\vec{v}) \left(\prod_{i=1}^{L+1} \int_0^\infty dt_i \exp\left(-\frac{t_i}{\tau_D}\right) \right) \\ &\times \left\langle \int_{-c}^c \dots \int_{-c}^c \frac{d^{L-V} u d^{L-V} s}{(\Sigma(E))^{L-V}} \prod_{\alpha=1}^V \frac{\exp\left(-\frac{t_{\text{enc}}^\alpha}{\tau_D} + \frac{i}{\hbar} \sum_{j=1}^{l_\alpha-1} s_{\alpha j} u_{\alpha j}\right)}{t_{\text{enc}}^\alpha} \right\rangle_{\Delta k} \\ &= \frac{1}{N_1 + N_2} \sum_{n=1}^\infty \left(\frac{1}{N_1 + N_2} \right)^n \sum_{\vec{v}}^{L-V=n} (-1)^V N(\vec{v}) \end{aligned} \quad (34)$$

with the $L + 1$ link times t_i . The (s, u) -integrals are calculated using the rule [28], that after expanding the exponential $e^{t_{\text{enc}}/\tau_D}$ into a Taylor series, only the t_{enc} -independent term contributes and yields in leading order in \hbar

$$\left\langle \frac{1}{\Sigma(E)} \int_{-c}^c \int_{-c}^c dsdu \exp\left(\frac{isu}{\hbar}\right) \right\rangle_{\Delta k} \sim \frac{1}{T_H} \quad (35)$$

with the so called Heisenberg time $T_H = \Sigma(E)/(2\pi\hbar)$. For the sum with respect to \vec{v} , one can derive recursion relations, yielding [28]

$$\sum_{\vec{v}}^{L-V=n} (-1)^V N(\vec{v}) = \left(1 - \frac{2}{\beta}\right)^n \quad (36)$$

with $\beta = 1$ and $\beta = 2$ for the case with and without time reversal symmetry, respectively. Relations of this kind are derived by describing our trajectories by permutations expressing the connections inside and between encounters and considering the effect of shrinking one link in an arbitrarily complicated structure to zero.

We then obtain for $T(E_F)$, given in Eq. (1), in the case with time reversal symmetry [29]

$$T(E_F)^{\beta=1} \approx \frac{N_1 N_2}{N_1 + N_2} + \frac{N_1 N_2}{N_1 + N_2} \sum_{n=1}^{\infty} \left(\frac{-1}{N_1 + N_2}\right)^n = \frac{N_1 N_2}{N_1 + N_2 + 1} \quad (37)$$

and in the case without time reversal symmetry

$$T(E_F)^{\beta=2} \approx \frac{N_1 N_2}{N_1 + N_2}, \quad (38)$$

which agrees with the diagonal contribution, already obtained in the previous section. Both results are in agreement with RMT predictions [31].

5 Semiclassical research paths: present and future

In the above sections we outlined the recently developed semiclassical techniques for treating off-diagonal contributions for one paradigmatic example of coherent transport, weak localization. Nonlinear (hyperbolic) dynamics as a prerequisite for the formation of correlated orbit pairs, together with classical ergodicity are at the core of the universality in the interference contribution to the ballistic conductance. Recently, this semiclassical approach to quantum transport has been extended along various paths, thereby gaining a more and more closed semiclassical framework of mesoscopic quantum effects:

In the presence of spin-orbit interaction, spin relaxation in confined ballistic systems and weak antilocalization, the *enhancement* of the conductance for systems obeying time-reversal symmetry (*i.e.* at zero magnetic field), has been semiclassically predicted [32] and generalized to other types of spin-orbit interaction [33] and higher-order contributions [34].

Ballistic conductance fluctuations, the analogue of the universal conductance fluctuations in the diffusive case, require the computation of semiclassical diagrams involving four trajectories. Again, RMT predictions could be confirmed

[25]. Accordingly, RMT predictions for shot noise in Landauer transport agree with recent semiclassical results [35]. This could also be shown for higher moments of the conductance in [36]. Even strong localization effects (in certain systems, *i.e.* chains of chaotic cavities) could be derived by making use of semiclassical loop-contributions [37].

Finally, beyond RMT, Ehrenfest time effects on transport properties have recently been in the focus of the field. As a result, ballistic conductance fluctuations turn out to be, to leading order, τ_E -independent [24], contrary to weak localization which is suppressed with $e^{-\tau_E/\tau_D}$ [23], as we have shown. Recently these results were extended to the ac-conductance in [38].

Beside universal spectral statistics of closed systems and transport through open systems, the semiclassical techniques have been recently generalized to decay and photo fragmentation of complex systems [39].

To summarize, by now there exists a newly developed semiclassical machinery to compute systematically quantum coherence effects for quantities being composed of products of Green functions. This opens up various possible future research directions: With respect to system classes, mesoscopic transport theory has been predominantly focused on electron transport, leaving the conductance of ballistic hole systems aside, which plays experimentally an important role and for which a semiclassical theory remains to be developed. The situation is similar for a novel class of ballistic conductors: graphene based nanostructures, see Fig. 2. More generally, a proper treatment of interaction effects in mesoscopic physics would probably represent the major challenge to future semiclassical theory.

To conclude, at mesoscopic scales where linear quantum evolution meets non-linear classical dynamics, further interesting phenomena can be expected to emerge, in view of increasingly controllable future experiments.

References

- [1] H.-J. Stöckmann, *Quantum chaos-an introduction* (Cambridge University Press, Cambridge, 1999).
- [2] M.C. Gutzwiller, *Chaos in Classical and Quantum Mechanics* (Springer, New York, 1990).
- [3] W.H. Miller, *Adv. Chem. Phys.* **25**, 69 (1974).
- [4] R. Blümel and U. Smilansky, *Phys. Rev. Lett.* **60**, 477 (1988).
- [5] R.A. Jalabert, H.U. Baranger, and A.D. Stone, *Phys. Rev. Lett.* **65**, 2442 (1990).
- [6] H.U. Baranger, R.A. Jalabert, and A.D. Stone, *Phys. Rev. Lett.* **70**, 3876 (1993).
- [7] K. Richter and M. Sieber, *Phys. Rev. Lett.* **89**, 206801 (2002).
- [8] O. Bohigas, M.J. Giannoni, and C. Schmit, *Phys. Rev. Lett.* **52**, 1 (1984).
- [9] H.U. Baranger, R.A. Jalabert, and A.D. Stone, *Chaos* **3**, 665 (1993).

- [10] K. Richter, *Semiclassical Theory of Mesoscopic Quantum Systems* (Springer, Berlin, 2000).
- [11] R.A. Jalabert, *The semiclassical tool in mesoscopic physics*, in: Proceedings of the International School of Physics Enrico Fermi, *New Directions in Quantum Chaos*, Course CXLIII, G. Casati, I. Guarneri and U. Smilansky (eds.), (IOS Press, Amsterdam, 2000).
- [12] S. Datta, *Electronic Transport in Mesoscopic Systems* (Cambridge University Press, Cambridge, 1995).
- [13] D.S. Fisher and P.A. Lee, Phys. Rev. B **23**, 6851 (1981).
- [14] J. Wurm, A. Rycerz, Ī. Adagideli, M. Wimmer, K. Richter, and H.U. Baranger, Phys. Rev. Lett. **102**, 056806 (2009).
- [15] S. Chakravarty and A. Schmid, Phys. Rep. **140**, 193 (1986).
- [16] For a derivation of a similar sum rule starting from ergodicity, see M. Sieber, J. Phys. A **32**, 7679 (1999).
- [17] M. Sieber and K. Richter, Physica Scripta **T90**, 128 (2001); M. Sieber, J. Phys. A **35**, L613 (2002).
- [18] A. Lassel, *Semiklassik jenseits der Diagonálnäherung: Anwendung auf ballistische mesoskopische Systeme*, diploma thesis, Universität Regensburg, (2003).
- [19] R.V. Jensen, Chaos, **1**, 101 (1991).
- [20] Ph. Jacquod and R.S. Whitney, Phys. Rev. B **73**, 195115 (2006).
- [21] B.V. Chirikov, F.M. Izrailev, and D.L. Shepelyansky, Sov. Sci. Rev. Sect. C **2**, 209 (1981).
- [22] I.L. Aleiner and A.I. Larkin, Phys. Rev. B **54**, 14423 (1996).
- [23] Ī. Adagideli, Phys. Rev. B **68**, 233308 (2003).
- [24] S. Rahav and P.W. Brouwer, Phys. Rev. Lett. **96**, 196804 (2006).
- [25] P.W. Brouwer and S. Rahav, Phys. Rev. B **74**, 075322 (2006).
- [26] M. Turek and K. Richter, J. Phys. A **36**, L455 (2003); M. Turek, *Semiclassics beyond the diagonal approximation*, PhD thesis, Universität Regensburg, (2004).
- [27] D. Spehner, J. Phys. A **36**, 7269 (2003).
- [28] S. Müller, S. Heusler, P. Braun, F. Haake, and A. Altland, Phys. Rev. Lett. **93**, 014103 (2004).
- [29] S. Heusler, S. Müller, P. Braun, and F. Haake, Phys. Rev. Lett. **96**, 066804 (2006); S. Müller, S. Heusler, P. Braun, and F. Haake, New J. Phys. **9**, 12 (2007).

- [30] P. Gaspard, *Chaos, Scattering and Classical Mechanics* (Cambridge University Press, Cambridge, 1998).
- [31] C.W.J. Beenakker, Rev. Mod. Phys. **69**, 731 (1997).
- [32] O. Zeitsev, D. Frustaglia, and K. Richter, Phys. Rev. Lett. **94**, 026809 (2005).
- [33] O. Zeitsev, D. Frustaglia, and K. Richter, Phys. Rev. B **72**, 155325 (2005).
- [34] J. Bolte and D. Waltner, Phys. Rev. B **76**, 075330 (2007).
- [35] P. Braun, S. Heusler, S. Müller, and F. Haake, J. Phys. A **39**, L159 (2006); R.S. Whitney and Ph. Jacquod, Phys. Rev. Lett. **96**, 206804 (2006).
- [36] G. Berkolaiko, J.M. Harrison, and M. Novaes, J. Phys. A **41**, 365102 (2008).
- [37] P.W. Brouwer and A. Altland, Phys. Rev. B **78**, 075304 (2008).
- [38] C. Petitjean, D. Waltner, J. Kuipers, Í. Adagideli, and K. Richter, *preprint*, arXiv:0906.1791.
- [39] D. Waltner, M. Gutiérrez, A. Goussev, and K. Richter, Phys. Rev. Lett. **101**, 174101 (2008); M. Gutiérrez, D. Waltner, J. Kuipers, and K. Richter, Phys. Rev. E **79**, 046212 (2009).